Miroslav Plavec
On the rotation effect in eclipsing binaries

Acta Universitatis Carolinae. Mathematica et Physica, Vol. 8 (1967), No. 1, 23--54

Persistent URL: http://dml.cz/dmlcz/142203

1967 ACTA UNIVERSITATIS CAROLINAE - MATHEMATICA ET PHYSICA No 1 Pag 23-54

On the Rotation Effect in Eclipsing Binaries

M. PLAVEC

Astronomical Institute, Ondřejov

(*Received November* 18, 1966)

Formulae are derived for the rotation effect on spectral lines of the Algol-like eclipsing binaries, observed during primary eclipses. Discussed are the rotation factor, representing the displacement of a line as a whole, and profiles of spectral lines. The finite intrinsic width of spectral lines is taken into account, and formulae are also given for linear limb darkening.

Numerical examples illustrate the application to actual eclipsing binaries. Represented are three cases: partial eclipses (Algol), total occultation (U Sagittae) and a transit eclipse with annular phase (YZ Cassiopeae). Results are shown by means of tables and diagrams. Problems of practical application are shown in more detail for the case of U Sagittae.

1. Introduction

Spectrographic observations of the Algol-type eclipsing binaries during eclipse are of considerable and manifold importance. Here under the name "Algol-type" we understand simply systems in which the secondary component is of so much a later spectral type that during the most part of the primary eclipse (naturally with the exception of the total occultation and closely adjacent phases of an advanced partial eclipse) the spectrum of the primary star is not seriously blended by the secondary spectrum, and its changes can be studied. In other words, the secondary star is assumed to act as a dark screen moving across the disk of the primary component.

Originally it was thought that these observations would lead straightforward to the determination of the rotational velocity of the primary and from it to its dimensions on the assumption that its rotation is synchronized with the period of revolution in the system. However, it has been found that just in the Algol-like systems deviations from synchronism occur and the primary components rotate as a rule faster that expected on the basis of synchronism. Thus this method for determining absolute dimensions is not reliable, but the non-synchronized rotation is such an interesting problem in itself that the determination of rotational velocities remains very important.

However, the phenomena observed during eclipses are often complex, since in

many systems the spectrum of the primary component is contaminated by circumstellar gaseous streams. These latter phenomena may be actually of even greater interest than rotation itself; however, in order to study them, we have again first to allow for pure effects of rotation.

Naturally we get much more information if we can study the line contours; in many cases, however, all that can be done is the measurement of the shift of a line as a whole, by setting the wire of the spectrocomparator on the optical centre of gravity of the line. In such a case, the interpretation of the observations prerequires the calculation of the rotation factor, which will be derived in section 4.

An analytical formula for the rotation factor was derived first by Petrie (1938) for the case of uniformly bright disks. Kopal (1942) was the first to point out that Petrie's formula admits of considerable simplification. Introducing his associated alpha functions, Kopal not only derived an elegant form, but also succeeded in solving the more general case of non-zero limb darkening. However, this elegant form has its drawbacks; it requires much more computation work, which can hardly be done on an automatic computing machine, since it involves an extensive use of special tables by Kopal and by Cesevič. Quite often, these tables are not available. All these complications are not warranted by the observations, which are usually not accurate enough to reveal the small difference between uniform disk and a disk with a certain degree of limb darkenning. Several test computations performed by J. Horn show that the differences are very small indeed.

We shall therefore return to Petrie's formula and derive in section 4 a new form, equivalent to the original one but simpler. It will be seen that the simplifications introduced by a different choice of variables are not merely formal; they make it possible to use one and the same formula for all possible cases of partial eclipses, contrary to Petrie's procedure. The application is easy and no special tables are required, as numerical examples will show. Also the derivation of the formula is shorter, and, I believe, more elegant.

Sections 6 and 7 deal with line profiles during eclipse. It is interesting to realize that this problem has not been seriously attacked until by Kopal in 1959. (Kopal, 1959). Kopal investigated only the problem of spectral lines that are intrinsically narrow, while here we shall treat actual lines, i.e. those of finite intrinsic width; in particular, Doppler– and Stark–brodened lines will be considered, although the formulae derived will be quite general.

Throughout the whole paper, we shall make the following fundamental assumptions: (1) The stars are spherical, (2) they rotate as rigid bodies, (3) their axes of rotation are perpendicular to the orbital plane, (4) their orbits are circular. In many systems these conditions are only nearly fulfilled, but in most cases the effect of the deviations can be expected to be small. Moreover, in case of (1) and (4) it can be further diminished by a sulitable choice of osculation elements.

In view of the fact that most of the actual observing material is of rather limited accuracy, it is proposed here to apply first the simple theory developed here, and

only if systematic and significant deviations are found, recourse should be made to more refined methods of analysis. Several papers have been published studying effects of non-sphericity of the stars (Kopal, 1959), differential rotation and inclined axes (Porfirjev and Kaleničenko, 1964; Hosokawa, 1953).

The great importance of detailed investigations of deviations from the simple model is obvious. But, first of all, we must have a consistent theory of the rotation effect fro the simple model and this is what is presented here. This theory is also fully sufficient for many present-day practical needs.

Effort has been made to make the formulae easily applicable for numerical computations. As these applications will most probably be made by students of eclipsing binaries, consistency was attempted in notation, formulation etc. with the current usage in the theory and practice of photometric studies of eclipsing binaries. Also the units were chosen according to this principle. Therefore also some of the formulae in sections 2, 3, and 5 are presented in a new form.

2. Formulae for Axial Rotation

Let us introduce a rectangular coordinate system with its origin at the centre of the primary component (the one being eclipsed at the primary minimum). The xy-plane is perpendicular to the line of sight, and the z-axis is positive towards the observer. Let the y-axis be the projection of the axis of rotation of the primary component onto the tangential plane. Then, according to our fundamental assumption (3), the x-axis joins the nodes of the relative orbit of the secondary component on the tangential plane. Let us take the x-axis positive in the direction of the ascending node (in the sense used in the theory of orbits of spectroscopis binaries: the star recedes from us at the ascending node). This implies that those points on the apparent disk of the primary have positive abscissae that are receding from us owing to axial rotation; also, the centre of the secondary (eclipsing) component has a positive x-coordinate after the primary mid-eclipse.

Consider first the axial rotation of the primary component. According to our assumption (3), the angle between the axis of rotation and the line of sight is equal to the inclination of the orbital plane of the binary, i. Thus the components of the vector of the angular velocity of rotation are

$$\vec{\omega} = [0; \omega \sin i; \omega \cos i] \tag{2.1}$$

Let an arbitrary point on the surface of the star have coordinates

$$\vec{r'} = [x'; y'; z']$$

The linear velocity of rotation of this point will be given by the vector product

$$\vec{V} = \vec{\omega} \times \vec{r'}$$

We can observe only the radial component of this velocity, i.e., its z-component. However, it is customary to take the radial velocity as positive when the object is receding from the observer; therefore the correct formula is

$$V_r(x') = x' \omega \sin i \tag{2.2}$$

Evidently the radial component of the velocity of rotation of any point on the stellar disk depends only on its x-coordinate in our reference frame.

Now an agreement must be made about the units. It is usual with the eclipsing binaries to take the radius of the relative orbit as unit of length; fractional radii of the components, expressed in terms of this unit, are denoted r_1 and r_2. The length A of the radius of the relative orbit itself is most conveniently expressed in terms of solar radii, $R_\odot$. Thus we can write

$$x' = x\, A\, R_\odot = 0.696.10^6\, A\, x\,, \tag{2.3}$$

and x' is now expressed in kilometres, while x is the dimensionless fractional coordinate defined in terms of the same unit as r_1.

The angular velocity of rotation can be written as

$$\omega = \frac{2\pi}{P_r}\,. \tag{2.4}$$

It is generally assumed that in most cases, the period of axial rotation P_r is equal to the period of orbital revolution, P. However, just in the best observed Algol-type binaries it has been shown that the primary components rotate in many cases considerably faster. We shall therefore introduce a factor of asynchronism, f, and write

$$\omega = \frac{2\pi f}{P}\,. \tag{2.5}$$

If the two periods P and P_r are equal (case of synchronism), then $f = 1$. If the primary rotates faster, $f > 1$.

The orbital period P is usually expressed in days. In order to get the radial velocity in (2.2) in km/sec, we must write the formula in the following form, using (2.3) and (2.5):

$$V_r(x) = \frac{2\pi f\, A\, R_\odot}{86\,400\, P}\, x \sin i\,, \tag{2.6}$$

or, inserting numerical values for the constants,

$$V_r(x) = 50.615\, \frac{f\, A}{P}\, x \sin i\,. \tag{2.7}$$

The extreme values of V_r correspond to $x = \pm r_1$. It is clear that the linear equatorial velocity of rotation of the star is

$$V_e = 50.615\, \frac{f\, A}{P}\, r_1\,, \tag{2.8}$$

so that (2.7) can be also expressed in the form

$$V_r(x) = \frac{x}{r_1} V_e \sin i \,. \tag{2.9}$$

This form is particularly useful in cases when we do not know the absolute dimensions of the system, but $V_e \sin i$ can be determined directly from the broadening of the spectral lines.

According to the Doppler principle, the displacement $\Delta\lambda$ corresponding to the radial velocity V_r is

$$\Delta\lambda = \lambda \frac{V_r}{c} = \frac{2\pi f A R_\odot \lambda}{86400\, c\, P} x \sin i \,, \tag{2.10}$$

or, inserting numerical values for the constants,

$$\Delta\lambda = 1.688 \,.\, 10^{-4} \frac{\lambda f A}{P} x \sin i \,. \tag{2.11}$$

The maximum value of this Doppler displacement is

$$\Delta\lambda_{\max} = 1.688 \,.\, 10^{-4} \frac{\lambda f A}{P} r_1 \sin i \,. \tag{2.12}$$

In these formulae, $\Delta\lambda$ and λ are to be expresssed in the same units, most conveniently in Angstroms.

3. Geometry of Eclipse

Fig. 3.1 shows the configuration of the two components at a moment t during ingress. The phase angle Θ, given by the well-known formula

$$\Theta = \frac{2\pi}{P} (t - t_0) \,, \tag{3.1}$$

where t_0 is the instant of the primary minimum (mid-eclipse), is negative. We can also assume, without loss of generality, that the centre of the secondary component projects into the second quadrant of the position angle φ, which we shall measure counterclockwise from the positive direction of the x-axis (see Fig. 3.1). Thus the coordinates of the (centre of the) eclipsing component are

$$x_0 = \sin \Theta = \delta \cos \varphi \tag{3.2}$$

$$y_0 = \cos \Theta \cos i = \delta \sin \varphi \,, \tag{3.3}$$

where the distance between the projected centres, δ, is given by the well-known formula

$$\delta^2 = \sin^2 \Theta \sin^2 i + \cos^2 i \,. \tag{3.4}$$

Let the radii of the two components be r_1 (eclipsed) and r_2 (eclipsing), respectively. We shall introduce, as is usual, the auxiliary variable s by writing (cf. Fig. 3.1.):

$$s = r_1 \cos \gamma ,$$

and then

$$r_2^2 = r_1^2 + \delta^2 - 2\,\delta\, s . \tag{3.5}$$

The coordinates of thes intersections of the two limbs are then

$$\begin{aligned} x_1 &= s \cos \varphi + q \sin \varphi & \qquad x_2 &= s \cos \varphi - q \sin \varphi \\ y_1 &= s \sin \varphi - q \cos \varphi & \qquad y_2 &= s \sin \varphi + q \cos \varphi \end{aligned} \tag{3.6}$$

where we have abbreviated $q = +(r_1^2 - s^2)^{\frac{1}{2}}$. The signs of the discriminants were chosen so as to make $x_1 \geqq x_2$. This means that $P_1\,(x_1, y_1)$ is the upper point of

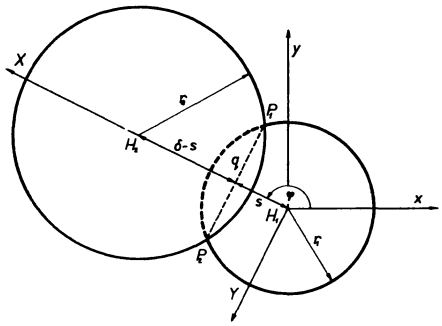

Fig. 3.1. Projected disks of the components at a phase near the beginning of eclipse.

intersection during ingress, but it is the lower point of intersection at egress, because then $y_1 \leqq y_2$.

The angle φ is determined by formulae (3.2) and (3.3); during ingress, $\frac{1}{2}\pi \leqq \varphi \leqq \pi$, while during egress, $0 \leqq \varphi \leqq \frac{1}{2}\pi$. The use of the angle φ in (3.6) can be avoided, since we can write

$$\sin \varphi = \frac{y_0}{\delta} , \quad \cos \varphi = \frac{x_0}{\delta} .$$

It should be noted that at egress the eclipsing component projects into the first quadrant of φ, and the phase-angle Θ is positive.

Mid-eclipse occurs when $\Theta = 0$. The coordinates of the eclipsing body are $x_0 = 0$, $y_0 = \delta = \cos i$; furthermore, $\varphi = \frac{1}{2}\pi$. If the eclipse even at this central phase is partial, the points of intersection remain real and are:

$$y_1 = y_2 = s, \; x_1 = -x_2 = (r_1^2 - s^2)^{\frac{1}{2}} . \tag{3.7}$$

However, if $|r_2 - r_1| > \delta$, the eclipse is complete: total for $r_2 > r_1$ and annular for $r_1 > r_2$. The complete eclipse lasts from the second contact Θ_2 to the third contact Θ_3; these phase angles are given by

$$\sin \Theta_{2,3} = \mp \frac{[(r_2 - r_1)^2 - \cos^2 i]^{\frac{1}{2}}}{\sin i} . \tag{3.8}$$

If the eclipse is total, our formulae for line profiles etc. to be derived in following sections naturally lose their sense, since the primary component is invisible. However, in case of an annular eclipse, the spectrum of the primary component never disappears completely, and special formulae must be derived for this phase.

For the sake of completeness, it should be remarked here that in general our formulae apply only to the intervals of phases $< \Theta_1, \Theta_2 >$ and $< \Theta_3, \Theta_4 >$, during which the system displays partial eclipse. The phases of the first and fourth contacts are given by

$$\sin \Theta_{1,4} = \mp \frac{[(r_1 + r_2)^2 - \cos^2 i]^{\frac{1}{2}}}{\sin i} . \tag{3.9}$$

Important for us is also the formula for the area (of the disk of the component under eclipse) eclipsed at any given moment. Elementary geometry offers us several possible formulae; for our purpose, the following one is probably the most convenient:

$$E = \frac{1}{2} \pi (r_1^2 + r_2^2) - r_1^2 \arcsin \frac{s}{r_1} - \delta (r^2{}_1 - s^2)^{\frac{1}{2}} - \\ - r_2^2 \arcsin \frac{\delta - s}{r_2} . \tag{3.10}$$

The uneclipsed (bright) portion of the disk has then an area $B = \pi r_1^2 - E$, or

$$B = \frac{1}{2} \pi (r_1^2 - r_2^2) + r_1^2 \arcsin \frac{s}{r_1} + r_2^2 \arcsin \frac{\delta - s}{r_2} + \delta q . \tag{3.11}$$

The advantage of these formulae lies in the fact that they apply to all phases of partial eclipses, disregarded whether $s < 0$ or $s > \delta$; it will be seen in the next section that this brings about a considerable simplification.

During the annular phase of a transit eclipse, the eclipsed area remains constant and is equal to the area of the smaller component;

$$E = \pi r_2^2, \text{ so that } B = \pi (r_1^2 - r_2^2). \tag{3.12}$$

If the disk of the primary is uniformly bright, the amount of light observed by the observer is proportional to the area $B(\Theta)$. If we take into account also limb darkening, proportionality no longer holds, and special tables must be used (e.g. Merrill, 1950) in order to calculate the instantaneous light of the primary $L_1(u, \Theta)$. It is no more possible to express L in terms of elementary functions for an arbitrary u. Using Merrill's tables for selected values of the limb-darkening coefficient u, we can write for the light of the primary at phase Θ, $L(u, \Theta)$,

$$L(u, \Theta) = \pi r_1^2 \left(1 - \frac{1}{3} u\right) [1 - \alpha^{oc}(k, p)], \tag{3.13}$$

if the eclipse is an occultation (larger star in front); and

$$L(u, \Theta) = \pi r_1^2 \left(1 - \frac{1}{3} u\right) [1 - \tau \alpha^{tr}(k, p) \tag{3.14}$$

for a transit (smaller star in front). Merrill's superscript x is equivalent to our u, $k = r_1/r_2$ for occultation and $k = r_2/r_1$ for transit, while

$$p = \frac{\delta - r_2}{r_1} .$$

4. The Rotation Factor

If it is not possible to study the actual profile of the spectral lines (because they are too narrow, faint or the dispersion is low), we can measure only the rotational displacement, during eclipse, of a line as a whole, by setting the wire of the spectrocomparator on the optical centre of gravity of the line. If we denote the observed displacement of the radial velocity from the extrapolated radial velocity curve (corresponding to the orbital motion) by V_r, we can write formally

$$V_r = F \, . \, V_e \sin i \, , \tag{4.1}$$

thus introducing the so-called rotation factor F. As can be seen by comparing (4.1) with (2.9), F represents a mean value of x/r_1, averaged over the uneclipsed portion of the disk of the primary. Thus we can write

$$F = \frac{\int\int I(x, y) \, x \, \mathrm{d}x \, \mathrm{d}y}{r_1 \int\int I(x, y) \, \mathrm{d}x \, \mathrm{d}y} , \tag{4.2}$$

where $I(x, y)$ describes the local surface brightness on the disk of the primary, and the integrals extend over the visible portion of its disk.

Now, when integrating over the whole uneclipsed area, it is advantageous to transform to another coordinate system in which the configuration during eclipse is always symmetrical with respect to the x-axis. This can be easily done, since it is only necessary to turn the axes x and y in the tangential plane by the angle φ, defined by (3.2) and (3.3). The new X-axis then always joins the centers of the two stars (cf. fig. 3.1), and we have

$$x = X \cos \varphi - Y \sin \varphi \, , \tag{4.3}$$

which can be substituted into (4.2). An immediate advantage of this transformation is that, in virtue of the above-mentioned symmetry,

$$\int\int Y \, I(X, Y) \, \mathrm{d}X \, \mathrm{d}Y = 0 \, ,$$

and (4.2) can be rewritten as follows:

$$F = \frac{\sin \Theta}{\delta \, r_1} \cdot \frac{\int\int I(X, Y) \, X \, \mathrm{d}X \, \mathrm{d}Y}{\int\int I(X, Y) \, \mathrm{d}X \, \mathrm{d}Y} . \tag{4.4}$$

However, if we want to obtain the final formula in terms of elementary functions, we must restrict ourselves to uniformly bright disks; for these, (4.4) can be simplified to

$$F = \frac{\sin \Theta}{r_1 \, \delta} \cdot \frac{\int\int X \, \mathrm{d}X \, \mathrm{d}Y}{\int\int \mathrm{d}X \, \mathrm{d}Y} . \tag{4.5}$$

The denominator is now simply the area of the uneclipsed portion of the disk of the primary; we need not perform the integration, since

$$\int\int \mathrm{d}X\,\mathrm{d}Y = B(\Theta)$$

as defined by formula (3.11) or (3.12), respectively.

Proceeding now to the evaluation of the integral in the numerator,

$$N = \int\int X\,\mathrm{d}X\,\mathrm{d}Y,$$

it is important to realize that, by virtue of symmetry, the contributions from any two surface elements placed symmetrically with respect to the Y-axis cancel each other. The integral is zero both for the whole uneclipsed disk and for central annular eclipse. Using this, we can proceed in a way best seen from Fig. 4.2, which

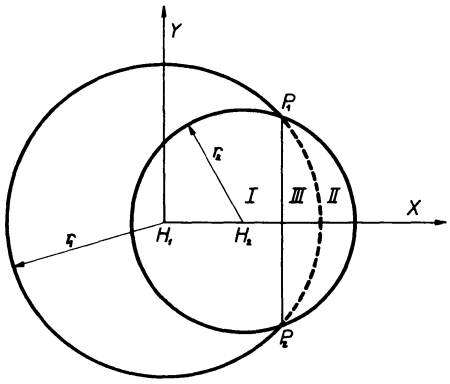

Fig. 4.2.

represents the configuration of the two stars at a moment during egress. We can first calculate the integral N_1 over the whole area of the disk of the secondary, and apply it with a negative sign; then we integrate over the area II between the chord P_1P_2 and the limb of the secondary (integral N_2), and eventually over the segment III bounded by the chord P_1P_2 and the limb of the primary to the right of this chord (N_3); then we shall have

$$N = -N_1 + N_2 - N_3\,. \tag{4.7}$$

N_1 is best calculated in polar coordinates with the pole at $X_0 = \delta$ (centre of the secondary), and with the polar angle α measured counterclockwise from the positive X-axis. We have

$$N_1 = \int_0^{2\pi}\int_0^{r_2} r\,(\delta + r\cos\alpha)\,\mathrm{d}r\,\mathrm{d}\alpha = \pi\,\delta\,r_2^2\,. \tag{4.8}$$

If the eclipse is complete and annular, $N = -N_1$. (4.9)

The integral N_3 is also easily calculated. First, we integrate along a horizontal line from $X = s$ to $X = +(r_1^2 - Y^2)^{\frac{1}{2}}$, and obtain

$$\int X\,\mathrm{d}X = \frac{1}{2}\,(r_1^2 - Y^2 - s^2)\,,$$

and the following integration is to be performed within the limits $-(r_1^2 - s^2)^{\frac{1}{2}}$ and $+ (r_1^2 - s^2)^{\frac{1}{2}}$. For the sake of convenience, let us write again

$$q = + (r^2 - s^2)^{\frac{1}{2}} .$$

Then the result of the second integration can be put down very simply as

$$N_3 = \frac{2}{3} q^3 . \tag{4.10}$$

The integral N_2 is somewhat intricate, because we must take care to derive a unique formula valid for cases when $s < \delta$, as well as for the phases of a transit eclipse when more than half of the disk of the secondary already projects on the disk of the primary, and $s > \delta$. Probably the best way to do it is to integrate first in vertical strips, between limits $\mp [r_2^2 - (X - \delta)^2]^{\frac{1}{2}}$; we obtain

$$\iint\limits_{\text{(area II)}} X \, \mathrm{d}X \, \mathrm{d}Y = 2 \int [r_2^2 - (X - \delta)^2]^{\frac{1}{2}} \, \mathrm{d}X ,$$

to be integrated between the limits $X = s$ and $X = \delta + r_2$. Substituting $w = X - \delta$, we can perform the integration easily, and obtain

$$\begin{aligned} N_2 = {} & \delta (\delta - s) [r_2^2 - (s - \delta)^2]^{\frac{1}{2}} + \frac{1}{2} \pi \delta r_2^2 + \\ & + \frac{2}{3} [r_2^2 - (s - \delta)^2]^{\frac{3}{2}} - \delta r_2^2 \arcsin \frac{s - \delta}{r_2} . \end{aligned} \tag{4.11}$$

However, the geometry of the configuration and formula (3.5) show that

$$[r_2^2 - (s - \delta)^2]^{\frac{1}{2}} = q .$$

Therefore,

$$N_2 = \delta (\delta - s) q + \frac{1}{2} \pi \delta r_2^2 - \delta r_2^2 \arcsin \frac{s - \delta}{r_2} + \frac{2}{3} q^3 .$$

The last term cancels out with the right-hand side of (4.10) when combined into N according to (4.7); the final formula becomes

$$N = \delta \left[(\delta - s) q - \frac{1}{2} \pi r_2^2 + r_2^2 \arcsin \frac{\delta - s}{r_2} \right] . \tag{4.12}$$

Inserting this into (4.5), we obtain for the rotation factor

$$F = \frac{\sin \Theta}{r_1} \cdot \frac{N'(\Theta)}{B(\Theta)} , \tag{4.13}$$

where

$$N'(\Theta) = q (\delta - s) - \frac{1}{2} \pi r_2^2 + r_2^2 \arcsin \frac{\delta - s}{r^2} ,$$

$$B(\Theta) = \frac{1}{2} \pi (r_1^2 - r_2^2) + r_1^2 \arcsin \frac{s}{r_1} + r_2^2 \arcsin \frac{\delta - s}{r_2} + q\delta$$

for any phase of partial eclipse. If the eclipse is complete and annular, equ. (4.9) and (3.12) apply, and we get a very simple formula:

$$F = \frac{\sin \Theta}{r_1} \cdot \frac{-r^2{}_2}{r_1^2 - r_2^2} \,. \tag{4.14}$$

From (4.14) we see immediately that F is positive during ingress (when $\Theta < 0$), negative during egress, and zero at mid-eclipse. But the same is true quite generally for all phases of the partial eclipse, to which formula (4.13) applies. The denominator $B(\Theta)$ is always positive because of its geometrical meaning. We shall now show that the numerator is always negative, thus making the sign of F always opposite to that of Θ. For the advanced phases of a transit eclipse, when $s > \delta$, this is easily seen, since all three terms combined into $N'(\Theta)$ are negative. When $\delta > s$, our reasoning can be based on geometrical arguments. From Fig. 3.1 we see that $(\delta - s)\, q$ represents the area of the triangle $H_2P_1P_2$. But substracted from it is the larger area of the sector $H_2P_1P_2$ (bounded by the limb of the secondary between P_1 and P_2); this area is given by the remaining two terms.

Let us now compare (4.13) with Petrie's form. In order to see the difference clearly, let us write down Petrie's formulae for the numerator in case of a transit. Petrie writes (in our notation)

Case I.: $\delta > s$:

$$\frac{N}{\delta} = -\left[q\,\frac{r^2 - \delta^2 - r_2^2}{\delta} + q\,(r_2^2 - q^2)^{\frac{1}{2}} + r_2^2 \arcsin\frac{q}{r_2}\right] . \tag{4.15}$$

Case II.: $s > \delta$:

$$\frac{N}{\delta} = -\left[q\,\frac{r^2 - \delta^2 - r_2^2}{\delta} - q\,(r_2^2 - q^2)^{\frac{1}{2}} + \pi\, r_2^2 - r_2^2 \arcsin\frac{q}{r_2}\right] . \tag{4.16}$$

Our introduction of s by means of (3.5) might appear as a mere formal simplification of the first right-hand terms; but, in fact, a systematic use of this variable makes it possible to avoid the ambiguities encountered by Petrie. Consider, for example, the second right-hand terms in (4.15) and (4.16). In Case I,

$$(r^2{}_2 - q^2)^{\frac{1}{2}} = \delta - s \,,$$

while in Case II,

$$(r_2^2 - q^2)^{\frac{1}{2}} = s - \delta \,.$$

Similarly, in Case I,

$$\arcsin\frac{q}{r_2} = \frac{1}{2}\pi - \arcsin\frac{\delta - s}{r_2} \,,$$

while in Case II,

$$\arcsin\frac{q}{r_2} = \frac{1}{2}\pi + \arcsin\frac{\delta - s}{r_2} \,.$$

It is clear that, using δ and s instead of q, we can write down a unique form of the right-hand terms of (4.15) or (4.16). In a similar way, another Petrie's ambiguity

is removed in the case of the denominator, where he had to distinguish between cases $s > 0$ and $s < 0$. Also, it is not necessary for us to distinguish between occultation and transit as long as the eclipse is not complete.

Example 4.1: Partial Eclipse - Algol

According to the catalogue by Kopal and Mrs. Shapley (1956), Algol has the following elements: $P = 2.86731$ days, $r_1 = 0.227$, $r_2 = 0.239$, $i = 82.°0$, $A = 15.7_{\odot}$. It is slightly more convenient to express phases as fractions of the period, $\Phi = \Theta/2\pi$, or in days, $\Phi^d = P \,.\, \Phi$. By (3.9), partial eclipse begins at $\Theta = -26.7°$, or at $\Phi = -0.074$. In equ. (3.8), $r_2 - r_1 < \cos i$, the eclipse is partial. Its ephemeris and the values of the rotation factor are given in Table 4.1. Note that from a certain phase of the eclipse, F begins to diminish again and is zero at mid-eclipse. It is unnecessary to continue the table through the phases of egress. It is easy to see that $\delta(\Theta) = \delta(-\Theta)$, $s(\Theta) = s(-\Theta)$, $B(\Theta) = B(-\Theta)$, $F(\Theta) = -F(-\Theta)$.

Table 4.1 *Rotation Effect of Algol*

Φ	δ	s	$B/\pi r_1^2$	F	V_r (km/sec)		
					$f = 0.6$	1	1.4
− 0.064	0.412	0.199	0.951	0.0433	1.6	2.7	3.8
− 0.056	0.369	0.177	0.883	0.0972	3.6	6.0	8.5
− 0.048	0.325	0.154	0.800	0.1569	5.9	9.8	13.7
− 0.040	0.283	0.132	0.708	0.2158	8.1	13.4	18.8
− 0.032	0.242	0.109	0.610	0.2655	9.9	16.5	23.2
− 0.024	0.204	0.089	0.514	0.2920	10.9	18.2	25.5
− 0.016	0.171	0.069	0.428	0.2715	10.1	16.9	23.7
− 0.008	0.148	0.055	0.365	0.1740	6.5	10.8	15.2
0	0.139	0.049	0.342	0	0	0	0
+ 0.008	0.148	0.055	0.365	− 0.1740	− 6.5	− 10.8	− 15.2

The three last columns in Table 4.1 give numerical values of the rotational component of the radial velocities, calculated by means of equ. (4.1), into which we inserted from (2.8). The equatorial velocity of rotation in case of synchronism is $V_e = 62.3$ km/sec; the actual velocity is probably not far from it.

Example 4.2: Annular Eclipse - YZ Cassiopeae

The elements, taken from the same catalogue as above, are: P = 4.46722 days, $r_1 = 0.1417$, $r_2 = 0.0769$, $i = 88.°2$, $A = 19.4_{\odot}$; therefore, synchronized $V_e = 31.15$ km/sec.

Partial eclipse begins at $\Phi = -0.0347$, annular phase begins at $\Phi_a = -0.0091$. For phases $|\Phi| < |\Phi_a|$, formulae (3.12) and (4.14) must be used instead of (3.11) and (4.13).

Table 4.2 *Rotation Effect of YZ Cassiopeae*

Φ	δ	s	$B/\pi r_1^2$	F	V_r (km/sec)		
					$f = 0.6$	1	1.4
− 0.032	0.202	0.136	0.986	0.0133	0.2	0.4	0.6
− 0.024	0.153	0.123	0.897	0.0886	1.7	2.8	3.9
− 0.016	0.105	0.120	0.782	0.1660	3.1	5.2	7.2
− 0.008	0.058	—	0.705	0.1477	2.8	4.6	6.4
0	0.031	—	0.705	0	0	0	0
+ 0.008	0.058	—	0.705	− 0.1477	− 2.8	− 4.6	− 6.4

Table 4.2 shows that the rotation effect in YZ Cas is small; this is because the eclipsing body is considerably smaller than the primary.

Example 4.3: Total Eclipse - U Sagittae

Elements by Kopal and Shapley are: $P = 3.3806184$ days, $r_1 = 0.210$, $r_2 = 0.278$, $i = 90.°0$, $A = 19.4_{\odot}$. Hence, if we assume synchronism, $V_e = 61.0$ km/sec.

First constact occurs at $\Phi = -0.0811$, occultation becomes total at $\Phi_t = -0.0108$. Ephemeris of the eclipse and the rotation factor are contained in Table 4.3. The rotation factor is much larger than in the two previous cases; $F \to 1$ as $\Phi \to \Phi^t$, i.e. F attains its maximum possible value. It can be shown that this maximum value is attained if and only if $i = 90°$ and the eclipse is total; for, in general, when $\Phi \to \Phi_t$, F approaches a limit given by the formula

$$F \to \frac{[r_2 - r_1)^2 - \cos^2 i]^{\frac{1}{2}}}{(r_2 - r_1) \sin i} . \tag{4.17}$$

Values of the rotation factor F are plotted against phase in Fig. 4.3 for the three systems considered here.

Table 4.3 *Rotation Effect of U Sagittae*

Φ	δ	s	$B/\pi r_1^2$	F	V_r (km/sec)		
					$f = 0.6$	1	1.4
− 0.080	0.482	0.206	0.998	0.0023	0.1	0.2	0.2
− 0.072	0.437	0.181	0.947	0.0491	3.0	4.2	5.4
− 0.064	0.391	0.153	0.863	0.1209	7.3	10.3	13.3
− 0.056	0.345	0.124	0.757	0.2078	12.7	17.7	22.8
− 0.048	0.297	0.093	0.634	0.3068	18.8	26.2	33.7
− 0.040	0.249	0.058	0.497	0.4168	25.4	35.6	45.8
− 0.032	0.200	0.017	0.352	0.5388	32.9	46.0	59.1
− 0.024	0.150	− 0.035	0.202	0.6772	41.3	57.8	74.3
− 0.016	0.100	− 0.115	0.061	0.8473	51.7	72.3	93.0
− 0.008	0.050	− 0.305	0.000	—	—	—	—

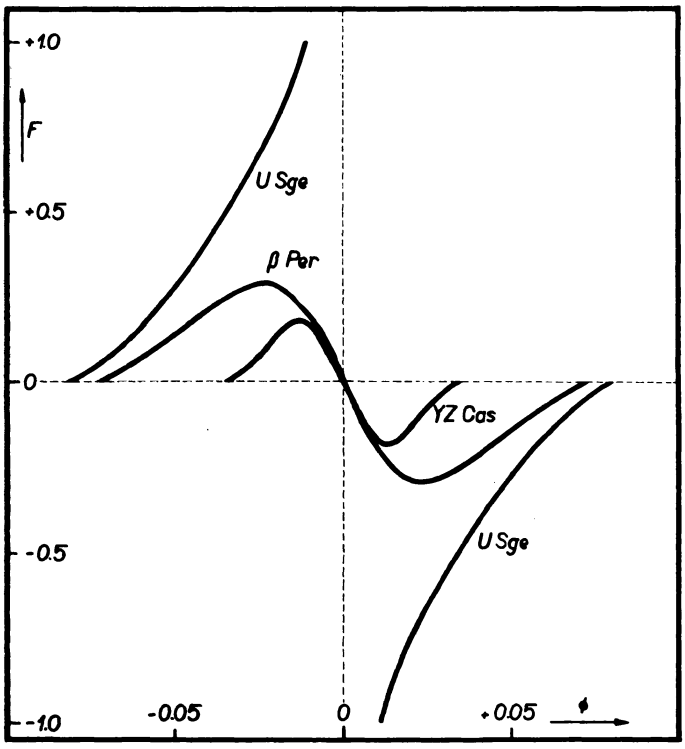

Fig. 4.3. Rotation factor F plotted against phase Φ (in fractions of period) for three systems.

Comparison with Observations of U Sagittae

U Sagittae is a system very suited for the study of the rotation effect, because the eclipse is total and the star is sufficiently bright. Struve (1949) secured an unusually rich material of 43 spectrograms during two consecutive eclipses on July 30/31 and August 1/2, 1949. The dispersion was 40 A/mm. Because the hydrogen lines and CaIIK are distorted by gas streams, Struve listed separately the radial velocities of the He I lines, and of all lines together except H and CaIIK. There is no systematic difference between these latter velocities and those of He I; therefore we shall use the values based on a greater number of lines.

Struve calculated the phases with the help of Jacchia's formula:

$$T_{\min} = \text{J. D. } 2417130.4151 + 3.3806184\,E + 0.0043 \sin (0.°107\,E + 266°), \quad (4.18)$$

but he remarks himself that the observed minima occured earlier than would be consistent with Jacchia's elements. From the intensities of the lines of the secondary component on his spectrograms, Struve concluded that the mideclipse actually occurred earlier by 0.028 day = 0.0082 P. This correction, however, appears at first sight somewhat too large. Irwin, observing two minima in October 1949 with a photoelectric photometer, obtained a correction of —0.0162 day to the linear formula

$$T_{\min} = \text{J.D. } 2417130.4170 + 3.3806184\,E\,. \quad (4.19)$$

Again, Svečnikov (1955) collected 14 minima of U Sge observed near the epoch of Struve's observations. Except for Irwin's observations, these are visual minima, and therefore Svečnikov quite correctly gives a much larger weight (100) to Irwin's normal minimum than to the other observations (1–5). No wonder, then, that Svečnikov's mean $O - C = -0.0151$ day does not differ materially from Irwin's result. The 13 visual observations show rather a large scatter between $O - C = -0.002$ and -0.027. Only this latter single observation supports Struve's correction; the average of the visual observations is -0.012 day.

Table 4.4 *Radial Velocities of U Sagittae at Eclipse*

Φ	V_0	V_r (km/sec) computed				
		$f = 1$	1.2	1.4	1.6	1.8
− 0.080	+ 28.1	+ 28.3	+ 28.3	+ 28.3	+ 28.3	+ 28.4
− 0.072	25.3	28.3	28.9	29.5	30.1	30.7
− 0.064	22.5	29.8	31.3	32.8	34.2	35.7
− 0.056	19.5	32.2	34.7	37.2	39.8	42.3
− 0.048	16.5	45.2	38.9	42.7	46.4	50.1
− 0.040	13.3	38.8	43.8	48.9	54.0	59.1
− 0.032	10.2	43.0	49.6	56.2	62.7	69.3
− 0.024	6.9	48.2	56.5	64.7	73.0	81.3
− 0.016	3.6	55.3	65.6	76.0	86.3	96.6
+ 0.016	− 10.0	− 61.6	− 72.0	− 82.3	− 92.6	− 103.0
+ 0.024	− 13.4	− 54.7	− 63.0	− 71.2	− 79.5	− 87.8
+ 0.032	− 16.9	− 49.7	− 56.3	− 62.9	− 69.5	− 76.0
+ 0.040	− 20.3	− 45.8	− 50.8	− 55.9	− 61.0	− 66.1
+ 0.048	− 23.8	− 42.5	− 46.2	− 50.0	− 53.7	− 57.5
+ 0.056	− 27.2	− 40.0	− 42.4	− 45.0	− 47.5	− 50.0
+ 0.064	− 30.6	− 38.0	− 39.5	− 40.9	− 42.4	− 43.9
+ 0.072	− 34.0	− 37.0	− 37.6	− 38.2	− 38.8	− 39.4
+ 0.080	− 37.3	− 37.4	− 37.5	− 37.5	− 37.5	− 37.6

Thus we can conclude that Irwin's result appears to be most reliable, and since the epoch of Struve's spectrographic observations precedes Irwin's only by two months, we believe that it is justified to calculate the phases of Struve's spectrograms with the help of the linear formula

$$T_{\min} = \text{J.D. } 2417130.4008 + 3.3806184\, E. \tag{4.20}$$

This is exactly the formula applied by McNamara (1951) in his paper on the spectrographic orbit of U Sagittae. McNamara's orbital elements are very reliable, and were used for computing the orbital-motion component of the radial velocity of the primary component during eclipse, V_0. Combined with the radial velocity due to rotation, V_r, (the latter calculated for several values of the factor of asynchronism f), they give the final predicted values of radial velocity listed in Table 4.4 and plotted in Fig. 4.4.

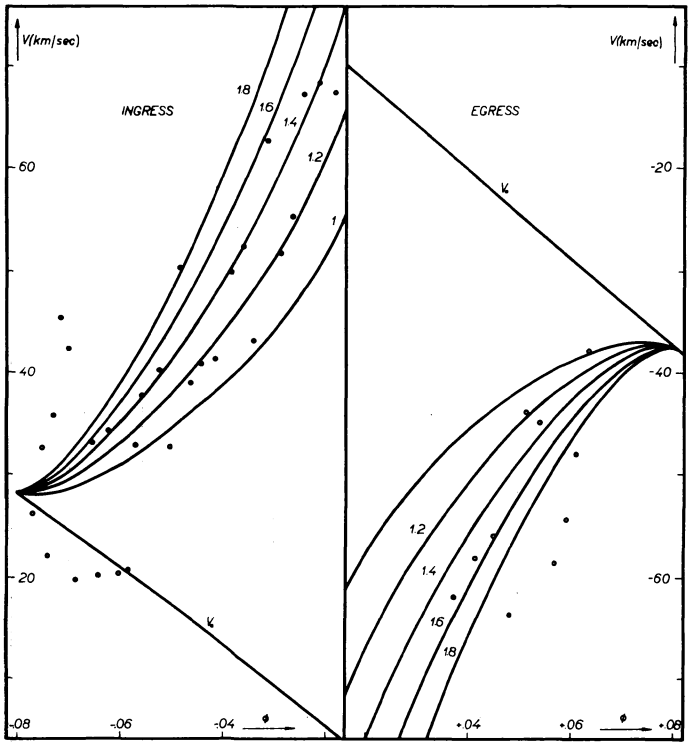

Fig. 4.4. Rotation effect in U Sagittae. Individual observations by Struve, and theoretical radial-velocity curves for several values of the parameter f.

Fig. 4.4 shows that even the observations of such an expert as Struve was show a very large scatter. This only supports my contention that the present-day observations do not warrant any more accurate theory. In order to derive a reliable value for the velocity of rotation, the observations were lumped into 9 normal points. Table 4.5 gives for these points the phase Φ, number of plates n, mean observed radial velocity V, and its mean error *m.e.*

Table 4.5 *Struve's Observations of U Sge – Normal Points*

Φ	n	V km/sec	m.e. km/sec ±
− 0.0742	5	+ 32.3	4.0
− 0.0651	6	+ 28.3	3.9
− 0.0548	5	+ 32.6	3.2
− 0.0452	4	+ 42.8	2.5
− 0.0349	4	+ 52.5	4.2
− 0.0236	5	+ 61.9	3.4
+ 0.0428	4	− 59.9	1.8
+ 0.0576	6	− 48.0	3.1
+ 0.0833	3	− 40.1	4.9

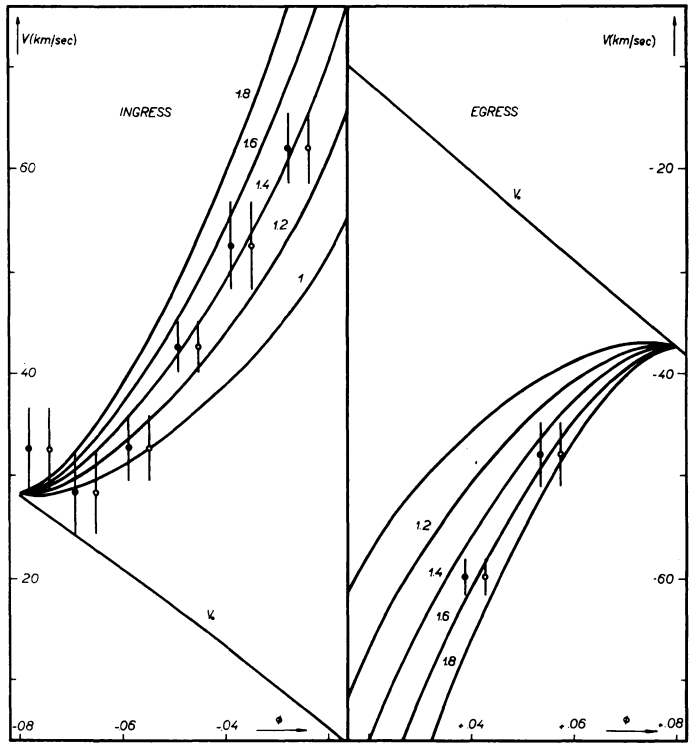

Fig. 4.5. Rotation effect in U Sagittae. Struve's observations – normal points.

The normal points together with their mean errors are plotted in Fig. 4.5; drawn are also curves representing the theoretical rotation effect. It is believed that the agreement between theory and observations in the more advanced stages of the eclipse (which are more important for the determination) is not bad. What is strange, however, is that for ingress the observations seem to be fairly well represented by the curve $f = 1.35$, approximately, while for egress the fit is decidedly better for $f = 1.7$. If we decrease the observed phases by about 0.004 P, the agreement between ingress and egress is much better, and the observations are fairly well represented by the curve $f = 1.5$ (se Fig. 4.5, full circles). This adjustment means that the correction to the linear ephemeris (4.19) was not —0.016 days as assumed after Irwin, but roughly —0.030 days, i.e. that, surprisingly enough, Struve was quite correct in his estimate in spite of all the photometric observations. Normal points with corrected phases are represented by full circles in Fig. 4.5.

With $f = 1.5$, the equatorial velocity of rotation of the primary component of U Sge turns out to be approximately 90 km/sec. Observations do not permit to state the result with more accuracy. Struve himself estimated 85 to 90 km/sec, although he considered a value as high as 100 km/sec as possible. Koch, Olson and Yoss (1965), studying the rotational broadening of lines outside eclipse, found $V_e = 76 \pm 12$ km/sec. From my plates, taken at Victoria with a dispersion of

10 A/mm (twice as high as the one used by the above-mentioned authors), J. Horn derived $V_e = 80$ km/sec. We can conclude that the primary component of U Sagittae rotates faster than it should in case of synchronism, but the deviation is not so large as e.g. in U Cephei.

5. Line Profiles Outside Eclipse

We shall now turn our attention to cases where we can study the profiles of the spectral lines. As has already been stated in section 1, we assume that the secondary, or eclipsing, star acts only as a dark screen, and does not cause blending of spectral lines. Moreover, we assume that the intrinsic profile does not vary across the disk of the primary. All this can be expressed otherwise and more accurately by saying that in our model, the distortion of the line contours during eclipse is entirely due to the fact that rotational broadening becomes asymmetrical, because part of the disk is eclipsed.

Before we begin with the investigation of the distortions during eclipse, we must derive formulae for rotationally broadened profiles outside eclipse. It is advantageous to return now to the coordinate system x, y, z used in sections 2 and 3, since in this coordinate frame the local radial velocity due to rotation, and the corresponding Doppler shift, are functions of the x-coordinate only.

Suppose now that, if the primary were non-rotating, the observer would receive a certain amount of radiation $I_0(\lambda_0)\,\mathrm{d}\lambda$ within the elementary interval of wavelengths between λ_0 and $\lambda_0 + \mathrm{d}\lambda$. Suppose now for a while that there is no radiation emitted at other frequencies. Now if the star rotates, the observer will see this radiation re-distributed over an interval of wavelengths $(\lambda_0 - \Delta\lambda_{\max}, \lambda_0 + \Delta\lambda_{\max})$, the width of which depends on $V_e \sin i$, and is given by formula (2.12):

$$\Delta\lambda_{\max} = 1.688 \,.\, 10^{-4}\, \frac{\lambda_0 f A r_1}{P} \sin i \,. \tag{5.1}$$

Consider now the radiation received at a wavelength λ lying inside this interval. If the stellar radiation is strictly monochromatic, as we assume, then all the radiation between λ and $\lambda + \mathrm{d}\lambda$ comes from the vertical strip between x and $x + \mathrm{d}x$ on the disk of the primary, where x and $\lambda - \lambda_0 = \Delta\lambda$ are connected by equation (2.11), or by the equivalent of it:

$$\frac{x}{r_1} = \frac{\Delta\lambda}{\Delta\lambda_{\max}} \,. \tag{5.2}$$

Before proceeding further, let us remark here that when formulating equations of this problem, it becomes increasingly awkward to use the symbols $\lambda - \lambda_0$ or $\Delta\lambda$, because we have to form differences of these differences. Let us therefore simplify the symbolism by introducing a new variable $Z = \lambda - \lambda_0$, which expresses

the distance in Ångstroms from the centre of the line. Writing conveniently $\Delta\lambda_{\max} = Z_m$, we can rewrite (5.2) into

$$Z = \frac{Z_m}{r_1} x . \tag{5.3}$$

Suppose now that the distribution of surface brightness at the given wavelength is described by a function $I(x, y)$. Then the amount of radiation received at the wavelength Z, expressed in terms of the total amount of radiation, will be described by the following function $F(x)$, which we shall call the broadening function:

$$F(x) = \frac{2 \int_0^{(r_1^2 - x^2)^{1/2}} I(x, y)\, dy}{2 \int_{-r_1}^{r_1} \int_0^{(r_1^2 - x^2)^{1/2}} I(x, y)\, dy\, dx} . \tag{5.4}$$

Let us now adopt the usual form of the law of limb darkening, namely

$$I(x, y) = I_0 (1 - u + u \cos \gamma) , \tag{5.5}$$

where the term involving the angle of foreshortening γ can be expressed in the form

$$\cos \gamma = \frac{z}{r_1} = \frac{1}{r_1} [r^2 - (x^2 + y^2)]^{\frac{1}{2}} . \tag{5.6}$$

Inserting from (5.6) into (5.5) and then into (5.4), we can evaluate the integrals in terms of elementary functions, and obtain

$$F(x) = \frac{6 (1 - u) (r_1^2 - x^2) + \frac{3 \pi u}{2 r_1} (r_1^2 - x^2)}{(3 - u) \pi r_1^2} . \tag{5.7}$$

For a uniformly bright disk, (5.7) reduces into an almost trivial formula

$$F(x) = \frac{2 (r_1^2 - x^2)^{\frac{1}{2}}}{\pi r_1^2} . \tag{5.8}$$

Formulae (5.7) and (5.8) are well-known, and are given in any textbook on astrophysics as formulae for the rotationally-broadened profile of an intrinsically monochromatic line. Only usually another variable is used, namely the distance along the x-axis expressed in terms of the stellar radius, $\xi = x/r_1$. We shall preserve our units, having in mind the application to the eclipses; but it will be useful to have the broadening function expressed in terms of Z instead of x. This is simple by virtue of (5.3); the formula reads

$$F(Z) = \frac{6 (1 - u) \left[1 - \left(\frac{Z}{Z_m}\right)^2\right]^{\frac{1}{2}} + \frac{3}{2} \pi u \left[1 - \left(\frac{Z}{Z_m}\right)^2\right]}{(3 - u) \pi Z_m} . \tag{5.9}$$

We can now pass over to real spectral lines, i.e. to lines with a finite intrinsic width. Let us assume that the intrinsic profile of a line is described by a function

$W(Z)$ of the wavelength difference $Z = \lambda - \lambda_0$. More precisely, let $W(Z)$ represent the depth of an absorption line, expressed as a fraction of the continuum at that wavelength. We suppose always that other factors affecting the position of the line have been allowed for; thus λ_0 is the tabular central wavelength of the line.

What will be the resulting depth $D(Z)$ of the line when rotational broadening applies? In order to answer this question, let us single out a wavelength Z'. If the star were non-rotating, the depth of the line at this point would be $W(Z')$.

Now, on the disk of the rotating star, only the radiation coming from the points on the y-axis remains undisplaced; the contribution to $D(Z')$ of an elementary strip along this axis will therefore be $F(0)\ W(Z)\ \mathrm{d}Z$. Radiation coming from a strip at x is displaced by an amount $Z(x)$ given by (5.3); therefore, its contribution to $D(Z')$ is $F(Z)\ W(Z' - Z)\ \mathrm{d}Z$. Integrating over the whole disk, we get

$$D(Z') = \int_{-Z_m}^{Z_m} F(Z)\ W(Z' - Z)\,\mathrm{d}Z\,. \tag{5.10}$$

Thus, in order to obtain the depth D of an absorption line at any one single point of the line profile, we have to perform an integration.

It is not necessary to make the transformation from x to Z; sometimes it is more convenient to have the formula (5.10) expressed directly in terms of x; it reads

$$D(Z') = \int_{-r_1}^{+r_1} F(x)\ W\left(Z' - \frac{Z_m}{r_1}\,x\right)\mathrm{d}x\,. \tag{5.11}$$

Our problem is now to find the laws $W(Z)$ of the intrinsic contours of the lines. For this purpose, spectra of three non-rotating stars were selected; α Lyr (A0V), α CMa (A1V), and o Peg (A1V). For all three, $V_e \sin i = 0$ according to Slettebak (1954). (It is in fact not accurate to call them non-rotating stars; they may be viewed pole-on). An examination of these spectra reveals that they contain essentially two types of line profiles. Weaker lines, as those of Fe I, Fe II, Ca I 4226 Å, and Mg II 4481 Å, can be described, to a fair degree of accuracy, by a Doppler contour:

$$W(Z) = C \exp\left[-(Z/d)^2\right], \tag{5.12}$$

where C is the central depth, and d can be obtained from the width of the line between the half-intensity points $W = \frac{1}{2}\,C$.

The Stark-broadened hydrogen Balmer lines have very broad intrinsic contours, which can be approximated by

$$W(Z) = \frac{1}{b + g\,|Z|^{5/2}} + C \exp\left[-(Z/d)^2\right]. \tag{5.13}$$

As a matter of fact, the outer wings conform very well to a simple $Z^{-5/2}$ formula, and most of the profile is well approximated by the first term on the right-hand side of (5.13), with two empirical constants, b and g. But a relatively very narrow Doppler core is superimposed, represented by the second term. The constant g

can be derived from the shape of the outer wings, and then b^{-1} is the extrapolated central depth of the pure Stark profile. A comparison with the actual depth gives C, and then d can also be found.

Inserting (5.12) or (5.13) into (5.10) or (5.11), we can calculate, point after point, the profiles of spectral lines broadened by the rotational effect. In the past, considerable effort was made to find approximate methods that would permit to calculate formulae like (5.10) with desk computers without too much trouble; cf., e.g., Unsöld (1955). The best thing to do at the present time is to perform the necessary numerical quadratures on a digital computer, as has been done in the following examples.

Example 1: Doppler profile

It has been found by our measurements that a mean profile representing well the MgII 4481 line in the three stars αLyr, αCMa, *o*Peg, is described by (5.12) with

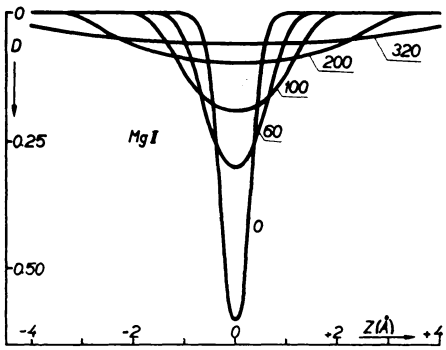

Fig. 5.1. Rotational broadening of Mg II 4481 Å. Depth of the line is plotted against wavelength; V_e sin i is expressed in km/sec.

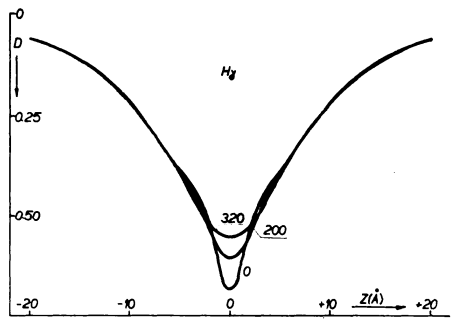

Fig. 5.2. Rotational broadening of Hγ.

$C = 0.60$, $d = 0.40$. The contours for five different values of V_e sin i (km/sec) are shown in Fig. 5.1.

Example 2: Stark profile

Again, we can represent $H\gamma$ in al the three stars fairly well by a mean profile, which, after J. Horn, has the following parameters: $b = 2.15$, $g = 0.008$, $C = 0.22$, $d = 1.9$, which are to be inserted into (5.13). Contours for three values of V_e sin i are in Fig. 5.2. Note that rotation changes only the central part of the profile (eliminates gradually the narrow central Doppler core), while the wings remain unchanged.

Because the spectral type of the three stars with V_e sin $i = 0$ is similar to the spectral type of the majority of the primaries of the Algol systems (B8–A2), we believe that the intrinsic profiles adopted here can be used in the discussion of the broadened and distorted profiles of the binaries.

6. Line Profiles at Eclipse – Uniformly Bright Disk

It has already been said that the line profiles become asymmetrical during eclipse because part of the disk is eclipsed, so that the purely rotational broadening effects is no more symmetrical. This means that, when performing the integration indicated in (5.11), we must bear in mind that, passing over the disk of the primary component from $x = -r_1$ to $x = +r_1$, the broadening function $F(x)$ changes not only its numerical value, but also its analytic form.

It is quite feasible to formulate the problem directly for the more general case of an arbitrary darkened disk. But is it more convenient to start with a uniformly

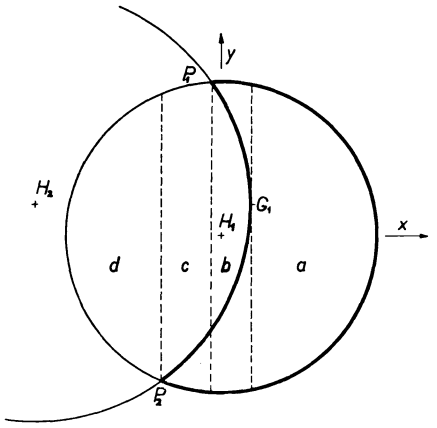

Fig. 6.1. Zones a–d on the disk of a partially eclipsed star.

bright disk, because the formulae are much simpler and the problem is clearer. Moreover, we have stated that in many practical applications, the assumption of a uniformly bright disk is a good approximation for the rotation factor, and the same is true for line profiles.

Thus, dealing with a uniformly bright disk, our task is to modify appropriately formula (5.4), which can now be written in a more general form as

$$F(x) = \frac{\mathcal{J}(x)}{B(\Theta)} \tag{6.1}$$

where $\mathcal{J}(x)\,\mathrm{d}x$ is the area of the visible part of an elementary vertical strip between x and $x + \mathrm{d}x$, while $B(\Theta)$ is the total area visible of the disk of the primary at a given phase Θ. These definitions are obvious generalizations of those introduced in section 5.

Now $B(\Theta)$ can be evaluated by means of equ. (3.11) and is constant for a given profile, i.e. for a given Θ. Our ask is therefore to study the function $\mathcal{J}(x)$. Fig. 6.1 represents the configuration at a phase of partial eclipse. We see that we can distinguish four regions on the disk of the primary.

In region (*a*), any elementary vertical strip is fully visible from its upper boundary at $+ (r_1^2 - x^2)^{1/2}$ to the lower boundary at $-(r_1^2 - x^2)^{1/2}$; thus we have

$$\mathcal{J}_a(x) = 2\,(r^2 - x^2)^{1/2}\,. \tag{6.2}$$

In region (*b*), the visible portion of an elementary vertical strip consists of two parts, bounded by the respective limbs of the two stars. Using again the symbols x_0, y_0 for the coordinates of the centre of the secondary (eclipsing component), we obtain, after a short algebra,

$$\mathcal{J}_b(x) = 2\{(r_1^2 - x^2)^{1/2} - [r_2^2 - (x - x_0)^2]^{1/2}\}\,. \tag{6.3}$$

Again, in the region (*c*), only the portion of the vertical strip is uneclipsed that lies between the lower limb of the secondary and the lower limb of the primary; we find

$$\mathcal{J}_b(x) = y_0 - [r_2^2 - (x - x_0)^2]^{1/2} + (r_1^2 - x^2)^{1/2}\,. \tag{6.4}$$

While this form of the broadening function is the most complicated, the following one is the simplest possible: for, in region (*d*), the vertical strips are completely eclipsed, and we have

$$\mathcal{J}_d(x) = 0\,. \tag{6.5}$$

Inserting now the appropriate form of $\mathcal{J}(x)$, as given by any of the equations (6.2) to (6.4), into (6.1), and from it again into (5.11), we can perform the numerical integration. Thus, for example, for the configuration shown in Fig. 6.1, we have

$$\begin{aligned} D(Z') = B^{-1}(\Theta)\Bigg[&\int_{x_2}^{x_1} \mathcal{J}_c(x)\; W\left(Z' - \frac{Z_m}{r_1}\right)\mathrm{d}x + \\ &+ \int_{x_1}^{x_0+r_2} \mathcal{J}_b(x)\; W\left(Z' - \frac{Z_m}{r_1}\right)\mathrm{d}x + \int_{x_0+r_2}^{r_1} \mathcal{J}_a(x)\; W\left(Z' - \frac{Z_m}{r_1}\right)\mathrm{d}x\Bigg]\,. \end{aligned} \tag{6.6}$$

As a matter of fact, we should write on the left-hand side $D(Z', \Theta)$, thus indicating that it is a function of phase, since the limits of the integrals on the right-hand side vary with phase. We see that we must make full use of the ephemeris of the eclipse as derived in section 3. We need to know the coordinates of the centre of the secondary, (x_0, y_0), as well as those of the points of intersection $P_1(x_1, y_1)$ and $P_2(x_2, y_2)$. Only the abscissae of these points appear explicitly in (6.6). However, we must consider the y-ccordinates, too, since the configuration in Fig. 6.1 is by no means the only possible; the zones (*a*) — (*d*) can be, under circumstances, situated in a different order, or they may be absent. There is a great variety of possible configurations depending on the photometric elements r_1, r_2, and i, and each case must be studied individually before we proceed to actual computations of the profiles.

An important role is played by the points $G_1(x_0 + r_2, y_0)$ and $G_2(x_0 - r_2, y_0)$ on the limb of the secondary. If either of them projects on the disk of the primary,

the zones (*b*) are present, otherwise not. Thus, in particular, if y_0 is always larger than r_1, regions (*b*) are absent during all phases of the eclipse. This condition can be formulated in a different way if we consider the configuration at mid-eclipse; with $\Theta = 0$, equ. (3.3) simplifies to $y_0 = \cos i$, and our condition can be stated as follows: If $\cos i > r_1$, zones (*b*) do not appear.

But the presence or absence of zones (*b*) is not the only possible cause of different configurations. Fig. 6.2 shows the course of events during the eclipse of

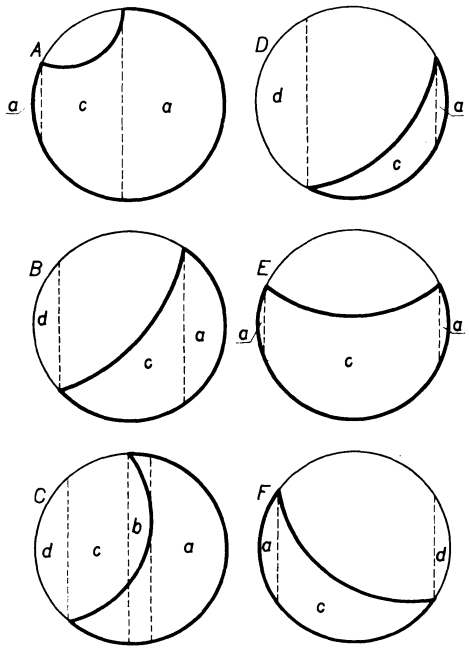

Fig. 6.2. Successive phases of primary eclipse of Algol (schematically – relative sizes and positions are not preserved).

Algol, which is typical for a number of other systems. Shortly after the secondary has encroached upon the disk of the primary, we have a configuration of the type *A*: there are two zones (*a*), and one zone (*c*). We can write down the intervals of x in the form of a small table:

Interval of x	*Kind of zone*
$-r_1 \leqq x \leqq x_2$	(*a*)
$x_2 \leqq x \leqq x_1$	(*c*)
$x_1 \leqq x \leqq r_1$	(*a*)

However, as soon as y_2 becomes negative, the first zone (*a*) changes into (*d*), the intervals remaining otherwise unchanged (configuration *B*).

When now the point G_1 enters on the disk of the primary, a zone (*b*) is interposed between (*c*) and (*a*); (*c*) extends now from x_2 to x_1 as before, but is followed by (*b*) between x_1 and $x_0 + r_2$, and (*a*) is restricted between $(x_0 + r_2)$ and r_1. This

configuration is shown Fig. 6.2*C*. It would not be difficult to describe qualilatively the changes in configurations during the whole eclipse. It is more important, however, to formulate quantitatively the equations determining the phases at which these changes in configuration occur.

The problem is to find phases

Θ_5, Θ_6 at which one of the points of intersection coincides with the point $(-r_1, 0)$;

Θ_7, Θ_8 at which the same happens for $(+ r_1, 0)$;

Θ_9, Θ_{10} at which the point $G_1(x_0 + r_2, y_0)$ coincides with one of the points of intersection;

Θ_{11}, Θ_{12} the same for $G_2(x_0 - r_2, y_0)$.

For this purpose, let us return to the equations (3.6) for the coordinates of the points of intersection. Eliminating q between the two equations of either pair, we obtain the equation of the chord in the form

$$x_0 x_1 + y_0 y_1 = s \delta , \tag{6.7}$$

and the same form for the other intersection. Again, making use of (3.5), we can rewrite (6.7) as follows:

$$\delta^2 + r_1^2 - r_2^2 - 2 (x_0 x_1 + y_0 y_1) = 0 , \tag{6.8}$$

a form identical for either of the points of intersection. As a matter of fact, equ. (6.8) is equation in one variable, namely Θ, which enters into δ through (3.4), and into x_0 and y_0 through (3.2) and (3.3), respectively. It is, however, more convenient to regard $x_0 = \sin \Theta$ as independent variable, and write the equation (6.8) in the form

$$x_0^2 \sin^2 i - 2 (x_0 x_1 + y_1 y_0) + r_1^2 - r_2^2 + \cos^2 i = 0 . \tag{6.9}$$

Here, it is true, y_0 is also a function of Θ, or of x_0. However, when looking for Θ_5 to Θ_8, we insert $y_1 = 0$, so that the term containing y_0 disappears. In order to avoid double indices, let us write for the while $x_0 = u$; we get two quadratic equations:

For $\Theta_{5,6}$: $\Theta_{5,6} = \arcsin u_{5,6}$ and u follows from

$$u^2 \sin^2 i + 2 r_1 u + r_1^2 - r_2^2 + \cos^2 i = 0 . \tag{6.10}$$

For $\Theta_{7,8}$: $\Theta_{7,8} = \arcsin u_{7,8}$ and u are roots of

$$u^2 \sin^2 i - 2 r_1 u + r_1^2 - r_2^2 + \cos^2 i = 0 . \tag{6.11}$$

In the equations determining the phases at which the points G_1 or G_2 fall on the limb of the eclipsed star, the factor at y_0 is not generally zero but y_0 again; however even here this variable can be eliminated. This is best seen when we return for a while to (6.8) and insert for x_1 and y_1 the coordinates of G_1 or G_2.

After a little algebra we get

for $\Theta_{9,10}$: $\Theta_{9,10} = \arcsin u_{9,10}$,

$$u^2 \sin^2 i + 2 r_2 u + r_2^2 - r_1^2 + \cos^2 i = 0 ; \tag{6.12}$$

for $\Theta_{11,12}$: $\Theta_{11,12} = \arcsin u_{11,12}$,

$$u^2 \sin^2 i - 2 r_2 u + r_2^2 - r_1^2 + \cos^2 i = 0 . \tag{6.13}$$

In all cases, the principal value of $\arcsin u$ is to be taken, for $-\frac{1}{2}\pi \leqq \Theta \leqq +\frac{1}{2}\pi$.

Numbering now the roots u_j so that we take first the discriminant with the positive sign and then with the negative sign, we see that $u_5 = -u_8$, $u_6 = -u_7$, and similarly $u_9 = -u_{12}$, $u_{10} = -u_{11}$. This is quite a natural result, since the eclipse is perfectly symmetrical with respect to phase $\Theta = 0$. Thus it is sufficient to solve only the equations (6.10) and (6.12), or the other pair.

Example 6.1: Partial eclipse - Algol

Equations (3.9), (6.10) to (6.13) give: $\Theta_1 = -26.7°$, $\Theta_5 = -25.0°$, $\Theta_9 = -24.8°$, $\Theta_{10} = -3.3°$, $\Theta_6 = -1.8°$. This means: Partial eclipse begins at $-26.7°$. The configuration corresponds to A in Fig. 6.2. At $-25.0°$, the lower point of intersection falls on the x-axis, configuration changes into B. At $-24.8°$, point G_1 begins to project on the disk of the primary, the configuration changes into C, which can be symbolically described as follows:

$$-r_1 < (d) < x_2 < (c) < x_1 < (b) < x_0 + r_2 < (a) < r_1 .$$

This situation lasts for most part of the ingress, until phase $-3.3°$; at this phase, point G_1 leaves the disk of the primary, and the distribution of zones in this configuration D is

$$-r_1 < (d) < x_2 < (c) < x_1 < (a) < r_1 .$$

At phase $-1.8°$, the point of intersection P_2 passes again through the point $x = -r_1$, $y = 0$, this time in the direction of positive y's. As Fig. 6.2E shows, zone (d) disappears and is replaced by (a), so that the configuration is

$$-r_1 < (a) < x_2 < (c) < x_1 < (a) < +r_1 .$$

After mid-eclipse, the course of events is symmetrically reversed: at phase $+1.8°$, P_1 passes through $(+r_1, 0)$ towards negative values of y_1, the configuration is

$$-r_1 < (a) < x_2 < (c) < x_1 < (d) < +r_1 ,$$

i.e. symmetrically reversed with respect to D, etc.

We are now able to write down the correct form of formula (6.1), using for individual intervals in x the appropriate formulae (6.2) to (6.5), respectivelly. These will be inserted into (5.11), and numerical integration can be performed, if we specify the law of the intrinsic line broadening, as described by the function $W(Z)$.

The line MgII 4481 shows the effect of rotational distortion very distinctly, being of small intrinsic width, and was therefore chosen for numerical computations. Its intrinsic profile was represented by the Doppler contour (5.12) with the same

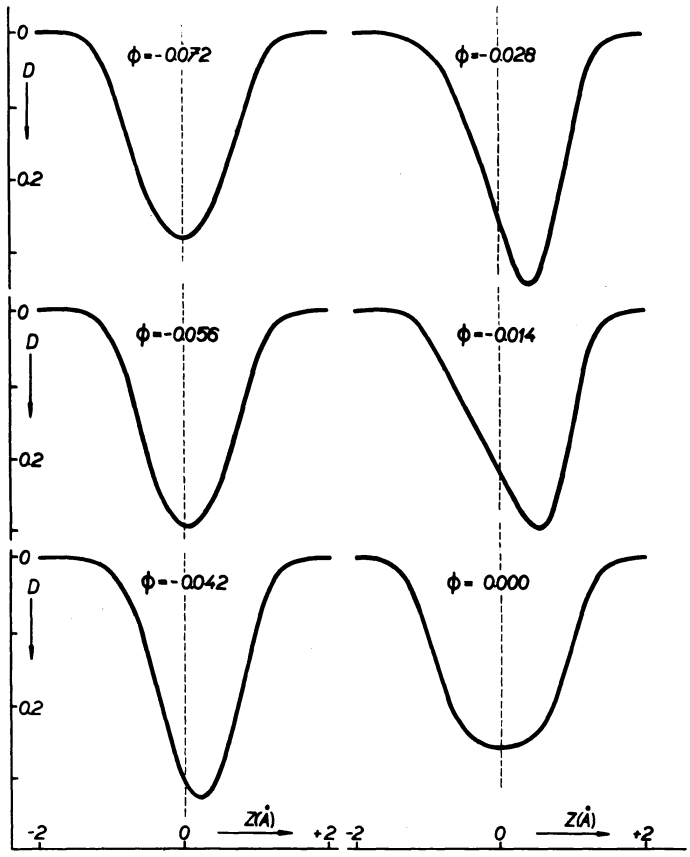

Fig. 6.3. Predicted variations in the profile of MgII in Algol during primary eclipse.

constants as in Example 5.1. Several profiles of this line at various phases of the eclipse are displayed in Fig. 6.3.

In the case of Algol, these computations can be well compared with observations. For example, the author of the present paper secured at Victoria a series of spectrograms with dispersion 5 Å/mm for this purpose. The interpretation, however, is more difficult, because the profiles are blended by lines due to the third component in the Algol system; therefore, the discussion is outside the scope of this paper.

Example 6.2: Annular Eclipse - YZ Cassiopeae

This system is also fairly bright, so that an analysis of the profiles is feasible, but nothing has been done so far. Our predicted profiles represent again the line

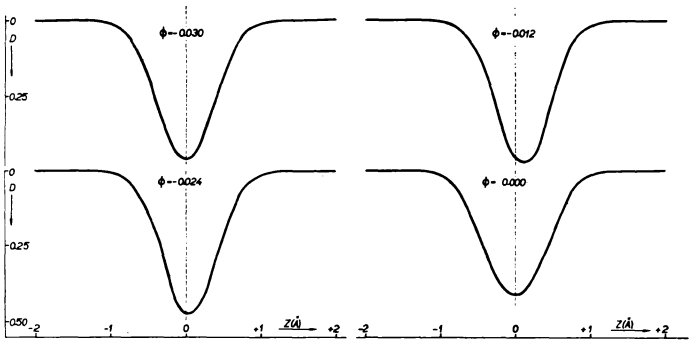

Fig. 6.4. Predicted variations in the profile of MgII in YZ Cas during primary eclipse.

MgII 4481 and vere computed – similarly as those for Algol — on the assumption that the rotation of the primary is synchronized with the period of revolution. The case is interesting because here we have a transit of a small secondary ($r_2 = 0.0769$) across the disk of a much larger primary ($r_1 = 0.1419$). The interest is, however, rather theoretical, since the distorsion of the line profiles is quite small, as Fig. 6. 4 shows.

Partial eclipse begins at phase —0.0347 P ($\Theta_1 = -12.°49$). Already at —0.0346, G_1 enters on the disk ($\Theta_{10} = -12.°45$), and at —0.0340 ($\Theta_6 = -12.°25$), P_2 crosses the x-axis and the configuration becomes of the well-known type C.

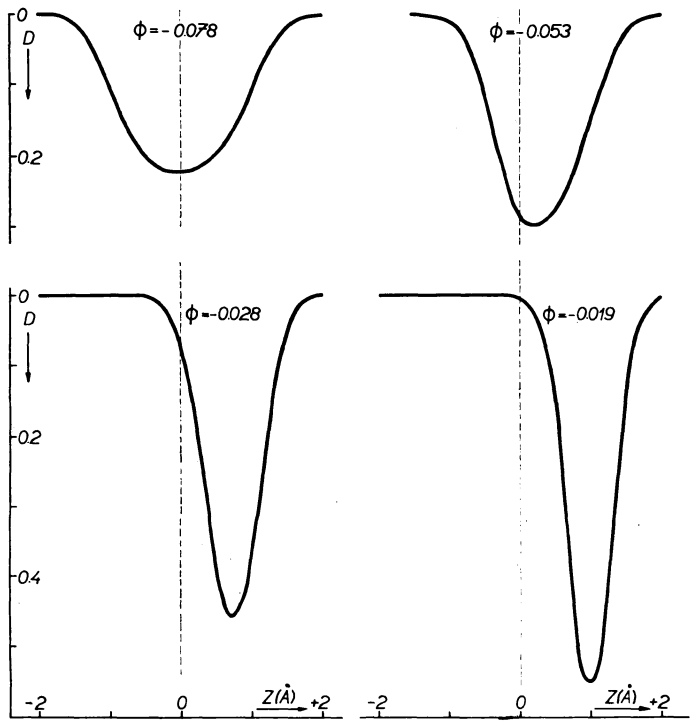

Fig. 6.5. Predicted variations of the profile of MgII in U Sagittae during primary eclipse.

What is new here is the situation after —0.0716 ($\Theta_5 = -4.°1$), when P_2 returns above the x-axis, and the configuration is

$$-r_2 < (a) < x_2 < (c) < x_1 < (b) < x_0 + r_2 < (a) < +r_1 .$$

Then, at phase —0.0097 ($\Theta_{12} = -3.°5$), the point G_2 already begins to project on the disk of the primary, and for a short while the configuration is

$$-r_1 < (a) < x_0 - r_2 < (b) < x_2 < (c) < x_1 < (b) < x_0 + r_2 < (a) < +r_1.$$

We have thus five zones, but already at the phase —0.0091 ($\Theta_2 = -3.°28$) the complete annular eclipse begins, the duration of which is 0.0182 P; during all this time, the configuration is $-r_1 < (a) < x_0 - r_2 < (b) < x_0 + r_2 < (a) < +r_1$. When calculating the profiles for this annular phase, B (Θ) is to be computed by (3.12).

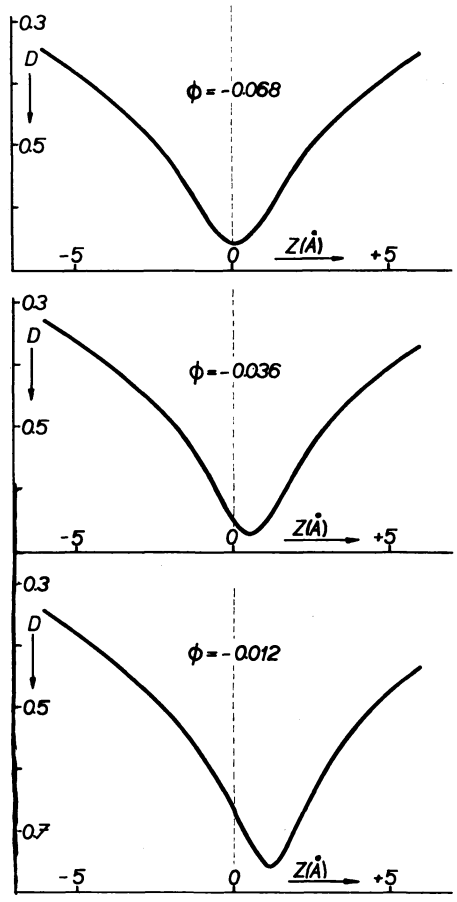

Fig. 6.6. Predicted variations of the profile of Hγ in U Sge during primary eclipse.

Example 6.3: Total Eclipse - U Sagittae

This case is very simple, since $i = 90°$. G_1 enters on the disk at the moment of the beginning of the eclipse, and during the whole ingress the configuration is the same, namely $-r_1 < (d) < x_2 = x_1 < (b) < x_0 + r_2 < (a) < +r_1$.

Several representative profiles of the MgII 4481 line are shown in Fig. 6.5. For this system, in which the rotational effect is particularly large because the eclipse is total, also the profiles of the line $H\gamma$ were computed. Its intrinsic profile was adopted in the form (5.13) and constants were chosen as in Example 5.2. Fig. 6.6 shows that the distortion of the hydrogen lines during eclipse is very small, because the intrinsic width is very large. Only the central parts of the line are affected to a certain degreee, the outer wings are practically quite unchanged.

The fact that the hydrogen lines are displaced as a whole but practically remain symmetrical is very important: it means that it should be possible to derive the rotational effect from their displacement as in the case of weak lines (cf. section 4, rotation factor); only the determination of the line centre will be as a rule less accurate. Actually, the rotational velocity of S Equ was so derived (Plavec, 1966).

7. Line Profiles at Eclipse – Disks with Limb Darkening

Passing now over to the more general case of disks with non-zero limb darkening, we can take over a great deal of the analysis from sections 5 and 6. The resulting depth of the absorption line in question at a given wavelength will be again given by formula (5.10), where the broadening function is again formally given by (6.1). However, the meaning of $\mathcal{J}(x)$ and $B(\Theta)$ must be generalized.

Suppose again that the distribution of surface brightness (at a given wavelength) over the disk of the primary is decribed by $I(x, y)$, and also that the intrinsic profile of the line in question is the same over the whole disk. Then, always considering radiation at a given wavelength within the line,

$$\mathcal{J}(x) = \int I(x, y)\, \mathrm{d}y\,, \tag{7.1}$$

where the integration extends over the visible part of the elementary vertical strip between x and $x + \mathrm{d}x$, and

$$B(\Theta) = \int\int I(x, y)\, \mathrm{d}y\, \mathrm{d}x\,, \tag{7.2}$$

where the integration extends over the whole visible portion of the disk of the primary. In other words, $F(x)$ is now the ratio of brightnesses, not of areas.

We assume again the usual linear law of limb darkening (5.5), but we shall write it directly in the form (5.6):

$$I(x, y) = I_0 \left[1 - u + \frac{u}{r_1} [r_1^2 - (x^2 + y^2)]^{1/2}\right]\,; \tag{7.3}$$

this function is to be inserted into (7.1) and (7.2).

It has already been said in section 3 that the total light of the uneclipsed area $B(\Theta)$ cannot be, for $u \neq 0$, expressed in terms of elementary functions. Special tables were prepared for this purpose (Merrill, 1950), giving the functions ${}^{u}\alpha^{oc}$, ${}^{u}\alpha^{tr}$ for $u = 0.1, 0.2, \ldots, 1.0$. Only for these particular values of u can our computations be performed. We have

$$B(\Theta) = I_0 \left(1 - \frac{1}{3} u\right) \pi r^2 (1 - \alpha) . \tag{7.4}$$

Only the last factor varies with Θ; let us call it $B'(\Theta)$.

Inserting now (7.3) into (7.1), and together with (7.4) into (6.1), we can write

$$F(x) = \frac{1}{B'(\Theta)} \left[\frac{3(1-u)}{3-u} \frac{1}{\pi r_1^2} \mathcal{J}(x) + \frac{3u}{3-u} \frac{1}{\pi r_1^3} K(x) \right] , \tag{7.5}$$

where

$$\mathcal{J}(x) = \int_{y_d}^{y_h} \mathrm{d}y = y_h - y_d , \tag{7.6}$$

$$K(x) = \int_{y_d}^{y_h} [r^2 - (x^2 + y^2)]^{1/2} \, \mathrm{d}y =$$

$$= \left| \frac{1}{2} y [r_1^2 - (x^2 + y^2)]^{1/2} + \frac{1}{2} (r_1^2 - x^2) \arcsin \frac{y}{(r_1^2 - x^2)^{1/2}} \right|_{y_d}^{y_h} . \tag{7.7}$$

The upper limit y_h and the lower limit y_d are expressed by different relations according to the zone in which the elementary strip in question lies.

Now the geometry of the problem is identical with that studied in detail in section 6; therefore we take over the zones (*a*), ..., (*d*) and calculate the integrals $\mathcal{J}(x)$ and $K(x)$ for each zone. But the formulae for $\mathcal{J}_a(x)$, ..., $\mathcal{J}_d(x)$ have already been derived in section 6, equations (6.2) to (6.5). We are left with integrals $K(x)$.

Because the elementary strips in zone (*d*) are completely eclipsed, we have, besides $\mathcal{J}_d(x) = 0$, also

$$K_d(x) = 0 . \tag{7.8}$$

In zone (*a*), the limits of integration are $y_h = +(r_1^2 - x^2)^{1/2}$, $y_d = -(r_1^2 - x^2)^{1/2}$. Inserting them into (7.7), we find

$$K_a(x) = \frac{1}{2} \pi (r_1^2 - x^2) . \tag{7.9}$$

In zone (*b*), the visible portion of the strip consists of two parts, with limits $y_h = +(r_1^2 - x^2)^{1/2}$ and $y_d = y_0 + \sqrt{r_2^2 - (x - x_0)^2}$, and again $y_h = y_0 - \sqrt{r_2^2 - (x - x_0)^2}$, $y_g = -(r_1^2 - x^2)^{1/2}$.

Inserting these limits into (7.7), we get

$$K_b(x) = \frac{1}{2}\pi(r_1^2 - x^2) + \frac{1}{2}(r_1^2 - x^2)\left[\arcsin\frac{y_0 - \sqrt{r_2^2 - (x - x_0)^2}}{(r^2 - x^2)^{1/2}}\right] -$$

$$- \frac{1}{2}(r_1^2 - x^2)\arcsin\frac{y_0 + \sqrt{r_2^2 - (x - x_0)^2}}{(r_1^2 - x^2)^{1/2}} +$$

$$+ \frac{1}{2}[y_0 - \sqrt{r_2^2 - (x - x_0)^2}]\,[r_1^2 - x^2 - [y_0 - \sqrt{r_2^2 - (x - x_0)}]^2]^{1/2} -$$

$$- \frac{1}{2}[y_0 + \sqrt{r_2^2 - (x - x_0)^2}]\,[r_1^2 - x^2 - [y_0 + \sqrt{r_2^2 - (x - x_0)^2}]^2]^{1/2}.$$

This is certainly an awkward formula, but an effort to bring it into a more manageable form failed.

Finally, for the zone (*c*), the limits are $y_h = y_0 - \sqrt{r_2^2 - (x - x_0)^2}$, $y_a = -(r_2^2 - x^2)^{1/2}$, and the formula is somewhat simpler:

$$K_c(x) = \frac{1}{4}\pi(r_1^2 - x^2) + \frac{1}{2}(r_1^2 - x^2)\arcsin\frac{y_0 - \sqrt{r_2^2 - (x - x_0)^2}}{(r_1^2 - x^2)^{1/2}} +$$

$$+ \frac{1}{2}[y_0 - \sqrt{r_2^2 - (x - x_0)^2}]\,[r_1^2 - x^2 - [y_0 - \sqrt{r_2^2 - (x - x_0)^2}]^2]^{1/2}. \qquad (7.11)$$

It is obvious that actual computations of line profiles at eclipse with non-zero limb darkening are much more time-consuming than in the case of uniformly bright disks.

References

1. HOSOKAWA Y., 1953: On the Rotation Effect of Velocity Curves. Publ. A. S. Japan, 5, 114
2. KOCH R. H., OLSON E. C., YOSS K. M., 1965: A Spectrographic Investigation of Some Bright Eclipsing Binaries, ApJ 141, 955
3. KOPAL Z., 1942: On the Rotation Factor, Proc. Nat. Ac. Sci. Washington 28, 133
4. KOPAL Z., 1959: Close Binary Systems, chapt. V., Chapman and Hall, London
5. KOPAL Z., SHAPLEY M. B., 1956: Catalogue of Elements of Eclipsing Binary Systems. Jodrell Bank Annals, 1/4, 141
6. MCNAMARA D. H., 1951: A Spectrographic Study of U Sagittae. ApJ 114, 513
7. MERRILL J. E., 1950: Tables for Solution of Light Curves, Contr. Princeton Obs. 23
8. PETRIE R. M., 1938: The Calculation of Rotation Factors for Eclipsing Binaries. Publ. D.A.O. Victoria 7, 133.
9. PLAVEC M., 1966: S Equulei, A New Close Binary with Gaseous Streams. BAC 17, No. 6
10. PORFIRJEV V. V., KALENIČENKO V. V., 1964: Issledovanije krivych lučevych skorostej. AŽ 41, 858
11. SLETTEBAK A., 1954: The Spectra and Rotational Velocities of Stars of Types B8-A2, ApJ 119, 146
12. STRUVE O., 1949: Spectroscopic Binaries. MN 109, 487.